ADVANCED ELECTRONIC MATERIALS
www.advelectronicmat.de

Electrical Characteristics of Field-Effect Transistors based on Chemically Synthesized Graphene Nanoribbons

*Ute Zschieschang, Hagen Klauk, Imke B. Müeller, Andrew J. Strudwick, Tobias Hintermann, Matthias G. Schwab, Akimitsu Narita, Xinliang Feng, Klaus Müellen, and R. Thomas Weitz**

The electronic properties of chemically synthesized graphene nanoribbons (GNRs) are investigated in a field-effect transistor (FET) configuration. The FETs are fabricated by dispersing GNRs into an aqueous dispersion, depositing the GNRs onto an insulating substrate, and patterning of metal contacts by electron-beam lithography. At room temperature, the GNR FET shows a large drain current of 70 μA, very good charge injection from the contacts, saturation of the drain current at larger drain-source voltages, and an on/off current ratio of 2. The small on/off current ratio can be explained by either the unfavorable transistor geometry or by the unintentional agglomeration of two or more GNRs in the channel. Furthermore, it is demonstrated that, by quantum-chemical calculations, the bandgap of a GNR dimer can be as small as 30% of the bandgap of a GNR monomer.

1. Introduction

The unusual electronic properties of graphene have spurred significant interest for its use in electronic devices, such as touchscreens, light-emitting diodes, sensors, and logic circuits.[1] In particular due to its high charge-carrier mobility and high saturation velocity, graphene is of great interest for use as the channel material in next-generation high-frequency transistors.[2] Application of graphene in field-effect transistors for digital device or circuit applications has, however, proven to be challenging. Due to the lack of a bandgap, graphene field-effect transistors display a current modulation ratio of typically less than 10, making them not useful for most applications. There is, however, a strategy to induce a bandgap into graphene, namely by shrinking one of its dimensions to below 10 nm, thus creating a graphene nanoribbon (GNR). Its bandgap is in general inversely proportional to its width, but depends also on the nature of the edges of the nanoribbon. Random defects at the edges or irregularities in the width of the nanoribbons result in uncontrollable variations in the electronic properties.

Experimental strategies for forming GNRs can be broadly categorized into top-down approaches and bottom-up approaches. Top-down techniques usually involve some form of subtractive patterning, cutting or unzipping of larger graphene entities or carbon nanotubes into GNRs. For example, electron-beam lithography and plasma etching techniques have been used to pattern GNRs to a width down to 10 nm from mechanically exfoliated[3,4] or epitaxially grown graphene.[5] As-fabricated GNRs showed the opening of an energy gap of about 0.14 eV at cryogenic temperatures. At room temperature, devices based on such top-down-produced GNRs with a width of about 10 nm have a current modulation ratio of less than 10, a high charge-carrier mobility of 1000 $cm^2\ V^{-1}\ s$, and large drain currents of 28 $mA\ \mu m^{-1}$.[5] The advantage of lithography-based GNR fabrication methods is their scalability to large wafer sizes using processes which are commonly applied in industrial protocols. Alternatively, GNRs as narrow as 3 nm produced by liquid exfoliation from graphene have been shown to have sizable bandgaps up to 0.4 eV and current modulation ratios in a field-effect transistor up to 10^7.[6] Finally, GNRs have also been produced by the unzipping of carbon nanotubes along their long axis.[7]

The main drawback of the abovementioned top–down methods is the poor reproducibility and limited control over the structure of the GNRs, especially with respect to their edge configuration, and this poses a high entry barrier for their application in electronic devices.[8] In contrast, bottom-up methods can reproducibly lead to GNRs of high structural perfection, i.e., with uniform width and edge termination and hence uniform electronic properties. Bottom-up GNR fabrication methods rely on synthetic organic chemistry and involve either surface-assisted or wet chemical strategies. With these methods, the most critical GNR parameters, including geometry, width, length, edge structure and mass of the repeating

Dr. U. Zschieschang, Dr. H. Klauk
Max Planck Institute for Solid State Research
Stuttgart, Germany
Dr. I. B. Müller
BASF SE, GVM/M, Ludwigshafen, Germany
Dr. A. J. Strudwick, Dr. T. Hintermann, Dr. M. G. Schwab
BASF SE, GVE/I Carbon Materials Innovation Center
Ludwigshafen, Germany
Dr. T. Hintermann
BASF Schweiz AG, Basel, Switzerland
Dr. A. Narita, Prof. X. Feng, Prof. K. Müllen
Max Planck Institute for Polymer Research
Mainz, Germany
Dr. R. T. Weitz
BASF SE, GVE/F, Ludwigshafen, Germany
E-mail: thomas.weitz@basf.com
Dr. R. T. Weitz
Innovation Lab GmbH
Heidelberg, Germany

DOI: 10.1002/aelm.201400010

unit, can be conveniently "written" into the graphene nanoribbon, leading in principle to predictable electronic properties. 1D GNR growth at surfaces is based on the reactive coupling of molecular precursors on single-crystalline metal substrates in ultra-high vacuum.[9,10] The electronic properties of such surface-grown GNRs have recently been measured after a poly(methyl methacrylate)-based transfer of the GNRs onto a Si/SiO_2 substrate.[10] Since the GNRs used for that study were less than 30 nm long, only devices based on random networks comprising a large number of GNRs were characterized. FETs based on such random GNR networks showed on/off ratios of 10^3 at room temperature, but very small on-state drain currents of less than 0.1 nA at a drain-source voltage of –1 V.[10] Surface-grown GNRs do have the advantage of atomic precision of the edges. However, GNRs produced by the surface-assisted approach are not easily dispersible in common liquids, and complex transfer methods are required in order to deposit the GNRs onto insulating device substrates. Such transfer usually leads to contaminants that degrade the electrical performance of the devices, and it also renders the large-scale integration of such GNRs challenging. Finally, such transfer processes typically result in unintentional doping with concomitant degradation of the electrical parameters.[11]

An alternative method for bottom-up GNR growth is their wet chemical synthesis.[12,13] Recently, ultralong GNRs functionalized with solubilizing hydrocarbon side chains have been successfully synthesized via a novel Diels-Alder protocol.[14] Dispersions of GNRs can be stabilized in organic solvents,[13,14] allowing for their easy deposition onto insulating substrates. FETs based on random networks of such bottom-up-synthesized and solution-deposited GNRs have recently shown on-state drain currents of up to 100 nA and an on/off ratio of 2 at a large drain-source voltage of –20 V.[15]

Here, we report on the successful transfer of bottom-up-synthesized GNRs onto insulating substrates from a water-based dispersion by established and scalable methods without the need for deposition steps assisted by organic solvents. We demonstrate the electrical characterization of GNRs having a length of several hundred nanometers in a field-effect transistor structure, showing on-state drain currents of up to 70 μA at a drain-source voltage of –1 V and on/off current ratios up to 2.

2. Experimental Section

Dodecyl-functionalized GNRs with a nominal length of 600 nm were synthesized following a previously described methodology.[14] The GNRs were dispersed in deionized water with 1 wt% of sodium dodecyl sulfate (SDS) as surfactant for stabilization. SDS is a surfactant that is commonly used for the dispersion and deposition of carbon nanotubes.[16] The dispersion was homogenized by tip sonication (20 pulses) and bath sonication (2 h) and finally centrifuged for 3 min at 10 000 rpm. Due to the small GNR concentration, the dispersion stayed clear during the entire process. Using fiber-optic quasi-elastic light scattering, we confirmed the presence of particles with a size of about 540 nm in the dispersion. To deposit the GNRs, degenerately doped silicon substrates with a gate-dielectric stack consisting of 100-nm-thick thermally grown SiO_2, 8-nm-thick Al_2O_3 grown by atomic layer deposition and a 1.7-nm-thick hydrophobic self-assembled monolayer of tetradecylphosphonic acid[17] were immersed into the water-based GNR dispersion for 12 h. Afterwards, the substrates were blow-dried with nitrogen, then rinsed with deionized water, and again blow-dried with nitrogen. Use of a hydrophobic SAM allowed for a better deposition yield of GNRs.[18] The GNRs were located by atomic force microscopy (AFM) and their location on the substrate was referenced against an array of pre-patterned alignment markers. An AFM image of a GNR and the metal alignment markers can be seen in **Figure 1**a. Finally, source and drain contacts were fabricated on GNRs by electron-beam lithography, deposition of 0.5-nm-thick Ti and 30-nm-thick AuPd (40/60), and lift-off of excess metal. The schematic transistor cross-section is shown in **Figure 2**.

3. Discussion

To confirm the presence and the chemical integrity of the GNRs on the substrate surface, Raman spectroscopy measurements with an excitation wavelength of 632.8 nm were performed on the same substrates on which the electrical measurements had been carried out. Figure 1b shows representative Raman spectra of two intact GNRs on the silicon substrate. The Raman spectra exhibit a G band position of ≈1608 cm^{-1} and a FWHM of ≈32 cm^{-1} which are comparable to those obtained in a previous report on bulk quantities or individual GNRs.[14,15] The FWHM is larger in the present work (compared to ≈25 cm^{-1})[14] due to the difference in laser excitation wavelength, which results in different excitations within GNRs and other confined graphene structures.[19] The Raman D band, observed at 1335 cm^{-1}, exhibits a high intensity. This is due to the confinement of the π-electrons within the GNR structure, a feature that is commonly observed within such systems.[19,20]

The transport properties of the GNRs were investigated by electrical measurements in which the doped silicon was used as a global gate electrode and the electric current through the GNRs was determined as a function of the applied gate-source and drain-source voltages. These experiments were performed in ambient air at room temperature. The transfer and output characteristics of a transistor with a lithographically defined channel length (L) of 100 nm can be seen in **Figure 3**, the AFM image of the GNR prior to contacting can be seen in Figure 1a. The current–voltage characteristics indicate a large on-state drain current of 70 μA at a drain-source voltage of –1 V. The output curves show excellent linearity at small drain-source voltages, which suggests that the current through the GNRs is not limited by the injection from the metal contacts. For drain-source voltages beyond about –200 mV, the onset of saturation of the drain current due to pinch-off of the carrier channel at the drain contact can be observed, which proves that the device operates as a field-effect transistor and which is an important prerequisite for digital device applications.

The width of the GNR measured by AFM is about 50 nm (Figure 1a). However, since it is well known that the lateral resolution of atomic force microscopy at such short length scales is limited by the finite radius of the AFM tip, we take the measured height of the GNR also as an estimate of its width.

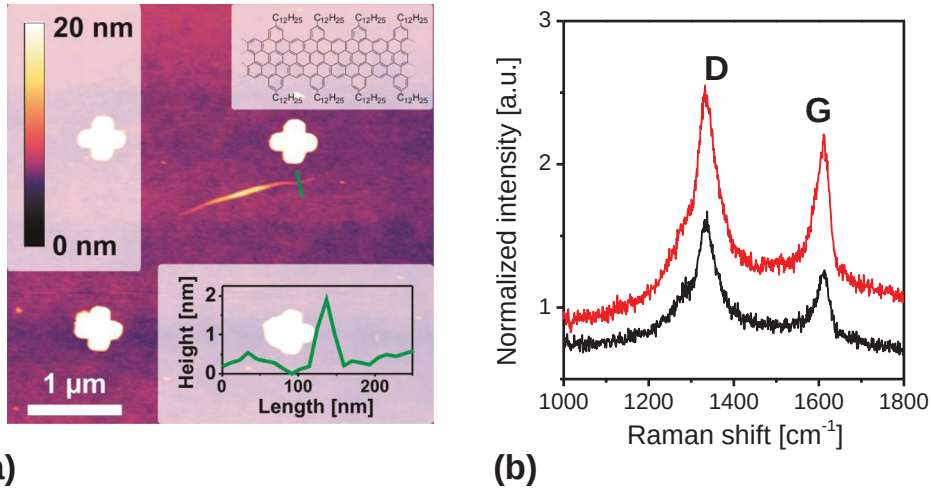

Figure 1. a) Atomic force microscopy (AFM) image of a chemically synthesized graphene nanoribbon (GNR) on a $Si/SiO_2/Al_2O_3$/SAM substrate. Alignment markers that are later used to align the source and drain contacts with respect to the GNR can also be seen. The slightly higher part of the GNR near its center is possibly due to remaining surfactant (SDS). Insets: Bottom: Height line trace at the position indicated by the green line. Top: Chemical structure of the GNR. b) Raman spectra of two isolated GNRs in two different locations on the same $Si/SiO_2/Al_2O_3$/SAM substrate. Characteristic Raman bands of the GNRs are observed at 1335 cm^{-1} (D band) and 1608 cm^{-1} (G band). These Raman spectra were taken with a 100× magnification optical lens, yielding a spot size of about 1 μm on the substrate surface. A neutral density filter was used to reduce the laser power on the substrate to less than 1 mW.

If we assume that the channel width of the transistor is identical to the width of an individual GNR, i.e., $W = 2$ nm, then the measured drain current of 70 μA corresponds to a width-normalized drain current (or current density) of 35 mA μm^{-1}, which is similar to the current density previously reported elsewhere[5] for top–down-fabricated GNR transistors. Using the same assumption ($W = 2$ nm), we extract a field-effect mobility of 500 $cm^2\ V^{-1}\ s$ from the transfer curve measured at a drain-source voltage of –1 V. However, from the AFM measurements alone it is not clear whether the transistor channel comprises an individual GNR or a small array of spontaneously agglomerated GNRs. Therefore, the values calculated for the charge-carrier mobility and the current density represent upper limits and should be taken with care.

The on/off current ratio is only about 2, which is smaller than what would have been expected based on the bandgap of 2 eV of the chemically synthesized GNRs.[14] The reason for the small on/off current ratio of the transistor is unknown, and we cannot rule out that it is related to short-channel effects,[21] due to the fact that the channel length is very short (about 100 nm). Also, as mentioned above, it is possible that the transistor channel consists not of an individual GNR, but of an array of two or more agglomerated GNRs.

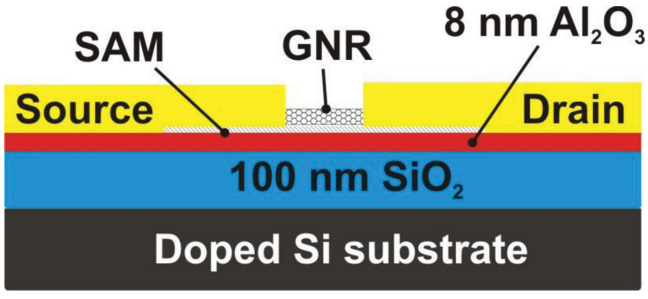

Figure 2. Schematic cross-section of the GNR-based field-effect transistor on which the electrical measurements were carried out. Ti/AuPd source and drain contacts were defined on the surface of a GNR by electron-beam lithography, metal evaporation, and lift-off.

To understand the impact of the agglomeration of two GNRs on the electronic properties of the transistor, we have performed quantum-chemical simulations of the band structure of two adjacent GNRs as function of their distance. We have based our calculations on VASP 5.2[22] using the PBE functional[23] in the PAW-form,[24] a cut off of 400 eV, and a k-point spacing below 0.25 1 $Å^{-1}$. Even though the PBE functional is known to underestimate energetic gaps (we find 1.48 eV for our GNR structure, while literature reports have calculated a gap of 2.05 eV,[25] we have chosen it for our calculation as we were interested in the impact of the agglomeration of GNRs on the bandgap and less so in the absolute value of the band structures. For this aim, the PBE functional as a member of the GGA family provides a much better result/calculation time ratio than hybrid functionals, which provide better absolute values. Results are displayed in **Figure 4**a. Since it is a priori not clear what lateral overlap adjacent GNRs would have, we have chosen three different lateral alignments, namely AA stacking, AB (Bernal) stacking, and one intermediate stacking, for our calculations. Cuts along the band structure for the three different stacking arrangements as well as an overview of the location of the smallest bandgap can be seen in Figure 4. Surprisingly, our calculations show that a GNR dimer does show a different bandgap compared with the individual GNR. The bandgap of the dimer can be as small as 30% (80%) of the initial bandgap in case two GNRs stack in the AA (AB) stacking motive at a graphite-like layer distance. In our experimental work, we have made every effort (e.g., sonication, centrifugation) to ensure that we have contacted an individual GNR. In principle, however, it is possible that we have contacted a GNR dimer with

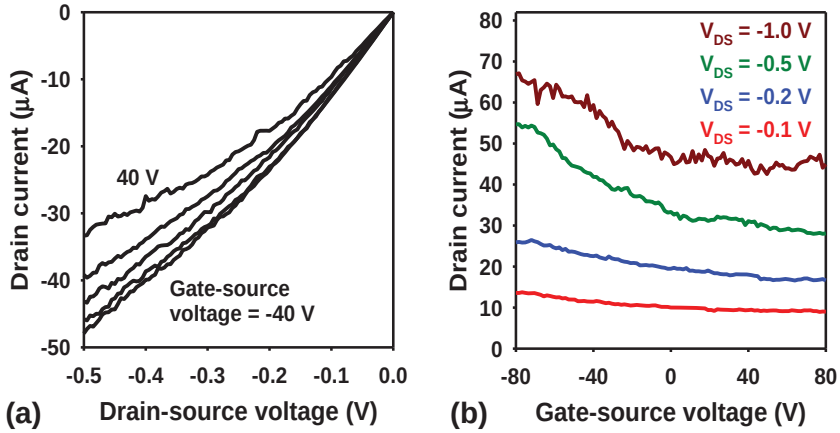

Figure 3. a) Output and b) transfer curves of the field-effect transistor that was fabricated using the GNR seen in Figure 1a. The transistor has a lithographically defined channel length of 100 nm. The output and transfer curves were measured in ambient air at room temperature.

concomitantly smaller bandgap, and it is therefore possible that the smaller on/off ratio is related to this smaller bandgap.

Summary

In conclusion, we have fabricated and characterized field-effect transistors based on GNRs. The chemically synthesized GNRs were deposited onto insulating substrates from a water-based dispersion for the first time, rather than from an organic solvent. This opens up the possibility of high-resolution, deterministic placement of the GNRs in specific, well-defined locations on the substrate surface, which is an essential prerequisite for future large-scale integration of GNRs into circuits.[26] Our GNR transistor shows large on-state drain currents (70 μA), good charge injection from the metal source and drain contacts, and current saturation at larger drain-source voltages. Except for the on/off current ratio, which is smaller than expected, the process we have demonstrated here fulfills all requirements for GNR integration into complex electronic circuits. We have taken various experimental measures (e.g., sonication, centrifugation) to ensure that our transistor indeed consists of one individual GNR. However, we cannot rule out that what we intended to be an individual GNR is in fact a spontaneously formed arrangement of a small number of GNRs. Nevertheless, even the characterization of a small array of GNRs would represent an important advance over previous reports of transistors that were based on random networks of a large number of GNRs[10,15] Using quantum-chemical calculations, we have demonstrated that the

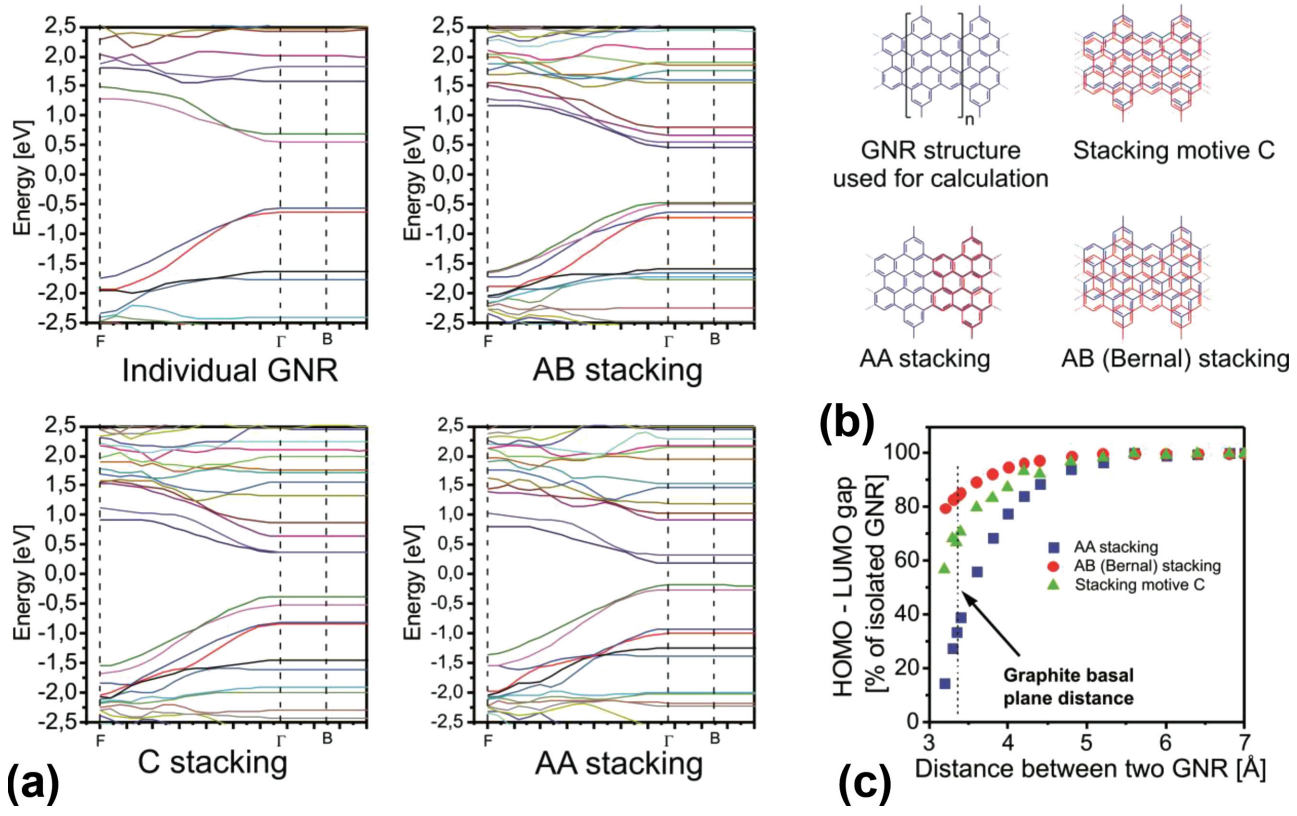

Figure 4. a) Band structure of an individual GNR (unit cell shown in (b)), and band structure of different GNR dimers with a GNR-to-GNR distance of 3.35 Å. b) GNR structure used for the calculation and different GNR dimer stacking motives. c) Calculated transport gap of three types of GNR dimers as a function of the intra-GNR distance.

bandgap of GNR dimers can be as small as 30% of the bandgap of individual GNRs, providing an explanation for the small on-off current ratio of our transistor. This would, however, not change the general conclusions of this study.

Acknowledgements

A.J.S. acknowledges financial support by a Marie-Curie Fellowship within the frame of the GENIUS project (FP7 – PEOPLE Programme).

Received: November 6, 2014
Revised: December 15, 2014
Published online: February 16, 2015

[1] A. K. Geim, K. S. Novoselov, *Nat. Mater.* **2007**, *6*, 183.
[2] F. Schwierz, *Nat. Nanotechnol.* **2010**, *5*, 487.
[3] M. Y. Han, B. Oezyilmaz, Y. Zhang, P. Kim, *Phys. Rev. Lett.* **2007**, *98*, 206805.
[4] Z. Chen, Y.-M. Lin, M. J. Rooks, P. Avouris, *Phys. E* **2007**, *40*, 228.
[5] W. S. Hwang, K. Tahy, P. Zhao, L. O. Nyakiti, V. D. Wheeler, R. L. Myers-Ward, C. R. Eddy Jr., D. K. Gaskill, H. Xing, A. Seabaugh, D. Jena, *J. Vac. Sci. Technol. B* **2014**, *32*.
[6] X. Li, X. Wang, L. Zhang, S. Lee, H. Dai, *Science* **2008**, *319*, 1229.
[7] a) D. V. Kosynkin, A. L. Higginbotham, A. Sinitskii, J. R. Lomeda, A. Dimiev, B. K. Price, J. M. Tour, *Nature* **2009**, *458*, 872; b) L. Jiao, L. Zhang, X. Wang, G. Diankov, H. Dai, *Nature* **2009**, *458*, 877.
[8] a) T. Wassmann, A. P. Seitsonen, A. M. Saitta, M. Lazzeri, F. Mauri, *Phys. Rev. Lett.* **2008**, *101*; b) V. Barone, O. Hod, G. E. Scuseria, *Nano Lett.* **2006**, *6*, 2748.
[9] J. Cai, P. Ruffieux, R. Jaafar, M. Bieri, T. Braun, S. Blankenburg, M. Muoth, A. P. Seitsonen, M. Saleh, X. Feng, K. Muellen, R. Fasel, *Nature* **2010**, *466*, 470.
[10] P. B. Bennett, Z. Pedramrazi, A. Madani, Y.-C. Chen, D. G. de Oteyza, C. Chen, F. R. Fischer, M. F. Crommie, J. Bokor, *Appl. Phys. Lett.* **2013**, *103*.
[11] M. Ishigami, J. H. Chen, W. G. Cullen, M. S. Fuhrer, E. D. Williams, *Nano Lett.* **2007**, *7*, 1643.
[12] a) J. S. Wu, L. Gherghel, M. D. Watson, J. X. Li, Z. H. Wang, C. D. Simpson, U. Kolb, K. Mullen, *Macromolecules* **2003**, *36*, 7082; b) L. Doessel, L. Gherghel, X. Feng, K. Muellen, *Angew. Chem. Int. Ed.* **2011**, *50*, 2540; c) T. H. Vo, M. Shekhirev, D. A. Kunkel, F. Orange, M. J. F. Guinel, A. Enders, A. Sinitskii, *Chem. Commun.* **2014**, *50*, 4172; d) T. H. Vo, M. Shekhirev, D. A. Kunkel, M. D. Morton, E. Berglund, L. Kong, P. M. Wilson, P. A. Dowben, A. Enders, A. Sinitskii, *Nat. Commun.* **2014**, *5*.
[13] M. G. Schwab, A. Narita, Y. Hernandez, T. Balandina, K. S. Mali, S. De Feyter, X. Feng, K. Muellen, *J. Am. Chem. Soc.* **2012**, *134*, 18169.
[14] A. Narita, X. Feng, Y. Hernandez, S. A. Jensen, M. Bonn, H. Yang, I. A. Verzhbitskiy, C. Casiraghi, M. R. Hansen, A. H. R. Koch, G. Fytas, O. Ivasenko, B. Li, K. S. Mali, T. Balandina, S. Mahesh, S. De Feyter, K. Muellen, *Nat. Chem.* **2014**, *6*, 126.
[15] A. N. Abbas, G. Liu, A. Narita, M. Orosco, X. Feng, K. Müllen, C. Zhou, *J. Am. Chem. Soc.* **2014**, *26*.
[16] L. Q. Jiang, L. Gao, J. Sun, *J. Colloid and Interface Sci.* **2003**, *260*, 89.
[17] U. Zschieschang, R. Hofmockel, R. Roedel, U. Kraft, M. J. Kang, K. Takimiya, T. Zaki, F. Letzkus, J. Butschke, H. Richter, J. N. Burghartz, H. Klauk, *Org. Electron.* **2013**, *14*, 1516.
[18] R. T. Weitz, U. Zschieschang, A. Forment-Aliaga, D. Kalblein, M. Burghard, K. Kern, H. Klauk, *Nano Lett.* **2009**, *9*, 1335.
[19] C. Castiglioni, M. Tommasini, G. Zerbi, *Phil. Trans. R. Soc. Lond. A* **2004**, *362*, 2425.
[20] a) C. Castiglioni, C. Mapelli, F. Negri, G. Zerbi, *J. Chem. Phys.* **2001**, *114*, 963; b) F. Negri, C. Castiglioni, M. Tommasini, G. Zerbi, *J. Phys. Chem. A* **2002**, *106*, 3306; c) F. Tuinstra, J. L. Koenig, *J. Chem. Phys.* **1970**, *53*, 1126; d) A. C. Ferrari, *Solid State Commun.* **2007**, *143*, 47.
[21] G. Baccarani, M. R. Wordeman, R. H. Dennard, *IEEE Trans. Electron Devices* **1984**, *31*, 452.
[22] a) G. Kresse, J. Hafner, *Phys. Rev. B* **1993**, *47*, 558; b) G. Kresse, J. Hafner, *Phys. Rev. B* **1994**, *49*, 14251; c) G. Kresse, J. Furthmuller, *Comput. Mater. Sci.* **1996**, *6*, 15; d) G. Kresse, J. Furthmuller, *Phys. Rev. B* **1996**, *54*, 11169.
[23] a) J. P. Perdew, K. Burke, M. Ernzerhof, *Phys. Rev. Lett.* **1996**, *77*, 3865; b) J. P. Perdew, K. Burke, M. Ernzerhof, *Phys. Rev. Lett.* **1997**, *78*, 1396.
[24] a) P. E. Blochl, *Phys. Rev. B* **1994**, *50*, 17953; b) G. Kresse, D. Joubert, *Phys. Rev. B* **1999**, *59*, 1758.
[25] S. Osella, A. Narita, M. G. Schwab, Y. Hernandez, X. Feng, K. Muellen, D. Beljonne, *ACS Nano* **2012**, *6*, 5539.
[26] H. Park, A. Afzali, S.-J. Han, G. S. Tulevski, A. D. Franklin, J. Tersoff, J. B. Hannon, W. Haensch, *Nat. Nanotechnol.* **2012**, *7*, 787.

